Short communication

Protonic membrane for fuel cell for co-generation of power and ethylene

Zhicong Shi, Jing-Li Luo[*], Shouyan Wang,
Alan R. Sanger, Karl T. Chuang

*Department of Chemical and Materials Engineering, #536, University of Alberta,
Edmonton, Alberta T6G 2G6, Canada*

Abstract

Yttrium-doped barium cerate, $BaCe_{0.85}Y_{0.15}O_{3-\alpha}$ (BCY15), membranes are proton-conducting electrolytes for intermediate-temperature protonic ceramic fuel cells (IT-PCFC), useful for, among other processes, co-production of power and ethylene by dehydrogenation of ethane. BCY15 membranes showed good conductivity at intermediate temperatures, 15 and 20 mS cm^{-1} at 700 and 750 °C, respectively. Maximum power density was 174 mW cm^{-2} at 700 °C, with a corresponding current density of 320 mA cm^{-2}, using a C_2H_6,Pt/BCY15/Pt,O_2 fuel cell, with a ca. 0.5 mm thick membrane, producing 34% ethane conversion with 96% ethylene selectivity Comparison of performances using vertical and horizontal set-ups showed that horizontal set-ups are subject to torsional strain, causing reduced cell performance resulting from even minor leakage at the glass seal.
© 2007 Elsevier B.V. All rights reserved.

Keywords: Protonic ceramic fuel cell; Dehydrogenation of ethane; Doped barium cerate ceramic; Glass sealant

1. Introduction

Conversion of alkanes to the corresponding alkenes is an industrially important process due to the high demand for feedstocks, and in particular for high purity alkenes for manufacture of polymers. Recently, intermediate-temperature proton ceramic fuel cells (IT-PCFC) which simultaneously produce value-added chemicals and electrical power gained much attention for their high energy conversion efficiency and low environment impact [1–3]. Previous research showed that direct hydrocarbon solid oxide fuel cells (SOFC) using oxygen ion-conductive solid electrolytes such as yttrium-stabilized zirconia (YSZ) can generate electrical power by conversion of hydrocarbon fuel to carbon oxides and water over the anode catalyst [4]. However, conventional YSZ-based SOFC require an operation temperature above 850 °C, which places severe demands on the materials used as interconnects and sealants. Interestingly, replacing the oxygen ion conductor by proton conductor in the fuel cell systems can bring significant potential advantages for selective conversion of hydrocarbons (Fig. 1) [5]. Firstly, no carbon oxides are generated in the anode chamber, because the proton-conducting electrolyte only permits the transfer of protons, and no oxygen is available for further reactions of the dehydrogenation product. Secondly, proton conduction implies that water vapor is produced at the cathode, where it is swept away by air, rather than at the anode (as in SOFC), where it dilutes the fuel. Thirdly, PCFC can be operated at intermediate temperatures with good electrochemical performance, which makes it easier to find suitable connection and sealing materials for these fuel cell systems.

To date, proton-conducting doped perovskites ($AB_{(1-x)}C_xO_{(3-\alpha)}$; A = Ca, Sr, and Ba; B = Ce and Zr; C = Sc, Y and lanthanides) are the most attractive solid electrolyte candidates for alkane dehydrogenation IT-PCFC. Partial substitution of tetravalent B ions by trivalent C ions (acceptor doping) in perovskites can introduce oxygen ion vacancies ($V_O^{\bullet\bullet}$). The exposure of these doped perovskites to either humid or hydrogen-containing atmospheres at elevated temperatures results in the incorporation of protons by reactions (1) and (2) [6]:

$$H_2O(g) + V_O^{\bullet\bullet} + O_O^{\times} \leftrightarrow 2OH_O^{\bullet} \tag{1}$$

* Corresponding author at: #536, Department of Chemical and Materials Engineering, University of Alberta, Edmonton, Alberta T6G 2G6, Canada.
Tel.: +1 780 492 2232; fax: +1 780 492 2881.
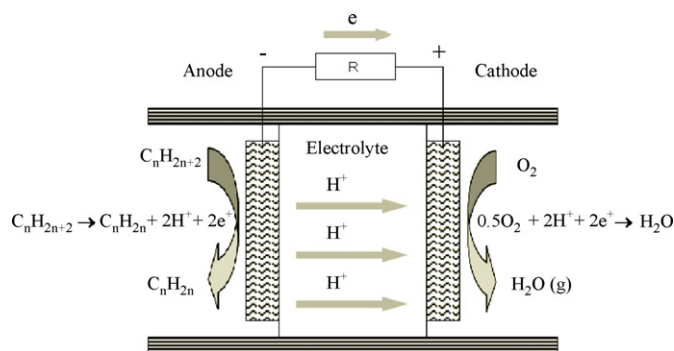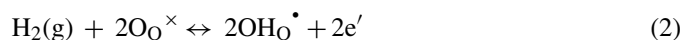*E-mail address:* jingli.luo@ualberta.ca (J.-L. Luo).

Fig. 1. Schematic of an intermediate-temperature proton ceramic fuel cell (IT-PCFC) using hydrocarbon as fuel.

$$H_2(g) + 2O_O^{\times} \leftrightarrow 2OH_O^{\bullet} + 2e' \tag{2}$$

The proton forms a covalent bond with a lattice oxygen, and migrates mainly as lone protons jumping between stationary oxide ions in oxides (Grotthuss mechanism), different from the mechanisms using proton transport by vehicles such as OH^-, H_2O, H_3O^+, and NH_4^+ in liquids and in solids with loosely bonded vehicles or open channels or layers (vehicle mechanism) [1]. The activation energy of proton hopping is at least 0.4 eV, which is assigned to activation of host and target oxygen ions [1].

Due to its high lattice constants and very small deviation from the ideal cubic perovskite structure, doped barium cerates show the highest proton conductivities among the family of proton-conducting perovskites: $BaCeO_3 > SrCeO_3 > BaZrO_3 > CaZrO_3$ [2]. Intense studies have been conducted into the stability of this class of materials in a high surface area powder form at high temperatures in a pure CO_2 atmosphere [7–11]. Unfortunately, the stability of doped and undoped $BaCeO_3$ is poor in CO_2 at elevated temperatures, though the reaction of BCY15 with CO_2 to form $BaCO_3$ is very slow in an atmosphere containing a relatively low partial pressure of CO_2 [12]. The stability of barium cerates can be increased when Ce atoms are partially substituted by Zr atoms because $BaZrO_3$ is chemically more stable than $BaCeO_3$ [13]. However, $BaZrO_3$ has much lower conductivity than $BaCeO_3$, and partial substitution by Zr resulted in lower proton conductivity.

In this paper, we describe a successful approach to apply protonic fuel cells for co-production of power and value-added products. Using ethane as a fuel, an IT-PCFC generates both electrical power and ethylene, with high selectivity, and this process has higher energy conversion efficiency when compared with current commercial technologies for direct catalytic dehydrogenation of ethane to ethylene in chemical reactors. We will also describe means for improving electrochemical performance, ethane conversion and ethylene selectivity by using a torsional stress free design set-up and a glass sealant instead of a ceramic sealant in a horizontal IT-PCFC. We also found that conventional sealants were prone to leakage under standard laboratory operational conditions. To our knowledge, only a few prior studies focused on glass–ceramic composite sealants [14,15] and glass sealant [16] for high temperature fuel cells. We will now demonstrate improved sealing of the

membrane using glass sealant in IT-PCFC using BCY15 as electrolyte.

2. Experimental

2.1. Material preparation and characterization

Polycrystalline powders of $BaCe_{0.85}Y_{0.15}O_{(3-\alpha)}$ (BCY15) were synthesized by solid-state reactions from stoichiometric $BaCO_3$ (Sigma–Aldrich, 99+%, A.C.S. reagent), CeO_2 and Y_2O_3 (nano-sized powders, both from Inframent Advanced Materials). Twenty-four hours ball-milled raw mixtures were calcined at 1400 °C for 10 h in air. The resulting materials were ball-milled again for 24 h, pressed at 30 MPa into discs with a diameter of 20 mm and a thickness of ∼2 mm, and sintered at 1550 °C for 10 h in air to obtain high-density membranes. Surface layers which may have contained impurities were removed by polishing, and the thickness was reduced to about 0.5 mm. Platinum paste (Heraeus Inc., CL11-5100) was applied to each side of the sintered discs with an area of ∼0.5 cm², and the discs were calcinated at 900 °C for 30 min before use for electrochemical measurements.

The yttrium-doped barium cerate series of electrolyte materials, $BaCe_{0.85}Y_{0.15}O_{(3-\alpha)}$ (BCY15) showed the highest conductivity in the temperature range of 550–800 °C. Hence we used BCY15 as electrolyte. The crystallinity of BCY15 was determined using powder X-ray diffraction (XRD) analysis using Rigaku Rotaflex X-ray diffractometer. The micro-structure and morphology of BCY15 membrane was investigated using scanning electron microscopy (SEM) technique with Hitachi S-2700 microscope. The micro-structures and compositions of used ceramic sealant (Aremco 503) and glass sealant (Aremco 617), both scratched from the fuel cell set-up after high temperature testing, were determined by SEM and energy-dispersive X-ray spectroscopy (EDS) analysis (Hitachi S-2700).

2.2. Fuel cell system fabrication

In our fuel cell set-up, platinum wires and meshes were used at both electrodes as output terminals and current collectors. The test station was designed for operation at temperatures as high as 900 °C with the fuel cell in either vertical or horizontal orientation. As described previously, the anode and cathode gas chambers were formed by placing the membrane electrode assembly (MEA) between concentric pairs of alumina tubes, and the assembly was heated in a Thermolyne F79300 tubular furnace [17]. All the above components were assembled and the assembly was supported using a stainless steel support, which was set on a frame with a rotational axis so the fuel cell set-up could be operated in horizontal or vertical orientation. The inner tube of each compartment extended from outside the heated reaction zone to a position close to the respective electrode of the cell. The outer perimeter of each outer tube was sealed to the membrane electrolyte with a thin layer of ceramic sealant (Aremco 503) at the cathode side, or with a thin layer of glass sealant (Aremco 617) at the anode side. To cure the sealants,

the furnace temperature was increased at a rate of $0.5\,°C\,min^{-1}$ to $110\,°C$, where it was kept for 2 h and then was increased to $871\,°C$ at a rate of $1\,°C\,min^{-1}$ and kept for 20 min. Then the furnace temperature was decreased to a set point for conducting the test. Nitrogen (Praxair, Grade 4.8) was fed into the anode chamber and extra dry oxygen (Praxair, Grade 2.6) was fed into the cathode chamber during sealant curing. After the cell had stabilized at the selected temperature, ethane fuel was introduced into the anode chamber. The system was maintained under these conditions for 30 min to stabilize before conducting measurements at each selected temperature. Pure C_2H_6 (Praxair, Grade 2.0) and extra dry O_2 were introduced into the anode and cathode compartments via the inner tubes, and after reactions in the fuel cell gases exited via the gas outlets in the outer tubes. All gas flows in fuel cell tests were controlled using mass flow controllers.

The Thermolyne F79300 tubular furnace had a uniform temperature zone ($\pm0.6\,°C$) in the central part of the cell. The temperature of the zone where the MEA was located during tests was monitored using a calibrated thermocouple to ensure consistency of readings in each test.

2.3. Electrochemical characterization

Cell open circuit voltage (OCV) was monitored as a function of time on stream. Data were recorded with a Solartron SI 1287 electrochemical interface and SI 1260 frequency response analysis instruments. When a steady OCV was reached, electrochemical impedance spectrum (EIS) measurements were performed in the frequency range 0.1 Hz to 1 MHz and ac amplitude of 10 mV to determine the cell resistance and conductivity of BCY15 electrolyte. Potentiodynamic measurements at a scanning rate of $5\,mV\,s^{-1}$ were conducted to determine the cell current–voltage curves from which the current density and power density were calculated.

2.4. Tests of ethane conversion and ethylene selectivity

The outlet gases from the anode chamber were analyzed online using a HP5890 Gas Chromatography with a packed column (OD: 1/8 in.; length: 2 m; Porapak QS) and a thermal conductivity detector (TCD).

3. Results and discussion

3.1. High temperature fuel cell set-up

A series of tests was conducted on a cell in horizontal orientation using, for example, sleeves containing a controlled atmosphere. These tests showed that performance improved when the atmosphere surrounding the seal contained no oxygen, indicating that leakage of external air through the seal affects the fuel cell performance. Thus we sought means to prevent formation of leaks through the seal.

We found that when the fuel cell set-up had vertical orientation, glass sealant could be beneficially used instead of ceramic sealant. In addition, in vertical orientation there was less tor-

sional strain, and consequently less propensity to cracking the sealant. Fuel cell performance was thereby improved by reducing the propensity for leakage of oxygen into the anode chamber. Apart from the influence of different sealants, we also wanted to determine if there were additional effects of cell orientation on fuel cell performance. Therefore, the fuel cell set-up had a rotational axis so that the fuel cell could be tested in either vertical or horizontal orientation.

3.2. Phase composition and micro-structure of BCY15

BCY15 perovskite was prepared using a solid-state reaction method. Its bulk structure and micro-structure, electrical conductivity and proton transport numbers were determined. XRD analysis proved that BCY15 powder calcined at $1400\,°C$ for 10 h comprised a single perovskite phase with good crystalinity [18]. SEM analysis (Fig. 2) showed that BCY15 membrane was very dense and formed by intimate contact BCY15 particles of 2–7 μm size, which favored fast conducting process by suppressing the impedance of grain boundary regions [2].

3.3. Conductivity of BCY15

Based on its high oxygen defect concentration, which incorporate protons upon exposure to humidity or H_2-containing atmospheres [19], BCY15 membranes provided good conductivity: 12, 15 and $20\,mS\,cm^{-1}$ at 650, 700 and $750\,°C$, respectively (Fig. 3). Thus the components of the reaction mixtures and surface intermediates in the anode (H_2, surface H species) and cathode (H_2O) compartments provided the necessary protons. The activation energy (E_a) of the mobility of protonic defects is 0.53 eV, which is typical of perovskite-type protonic conductors [1]. The ion conductivity of BCY15 in intermediate-temperature region is comparable with that of 8% yttria stabilized zirconia (8YSZ), the most used electrolyte currently used in SOFC, which is in the range of 10 and $15\,mS\,cm^{-1}$ at $700\,°C$ [20,21]. Therefore, BCY15 is a promising candidate for use as electrolyte in intermediate-temperature fuel cells.
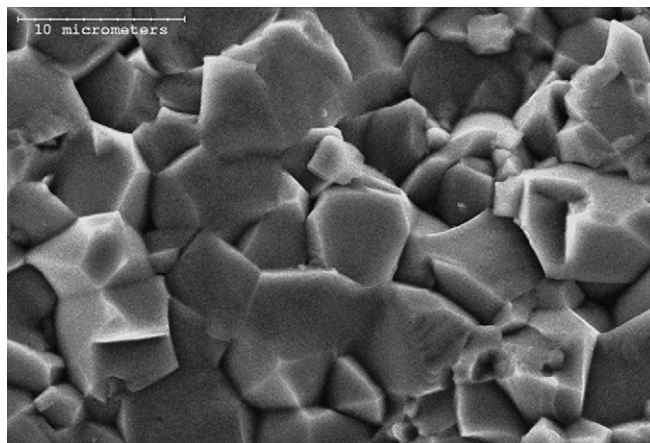

Fig. 2. Cross-sectional scanning electron microscopy (SEM) of $BaCe_{0.85}Y_{0.15}O_{(3-\alpha)}$ (BCY15) sintered in air at $1550\,°C$ for 10 h.
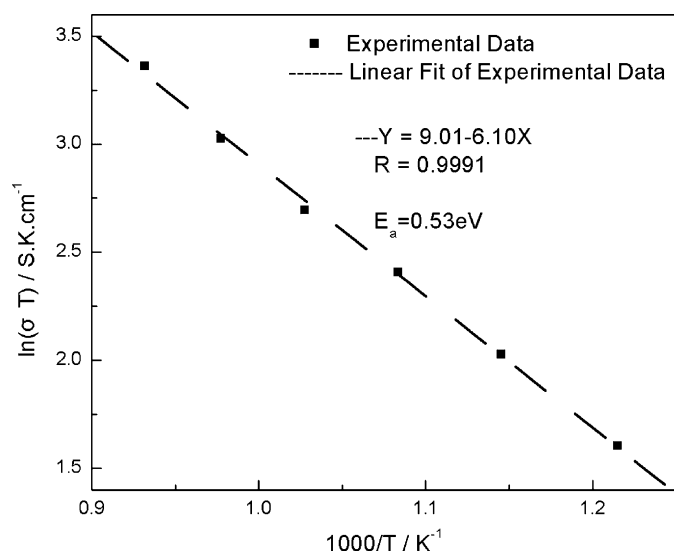
Fig. 3. Conductivity–temperature curves for $BaCe_{0.85}Y_{0.15}O_{(3-\alpha)}$ (BCY15) ceramic membrane tested at fuel cell operating temperatures and open circuit condition. E_a is activation enthalpy of the mobility of protonic defects.

Although BCY is a mixed ion conductor [22], oxygen ion conductivity is sufficiently low that it does not affect cell performance under the present operating conditions [18].

3.4. Enhanced performance of vertically oriented IT-PCFC

C_2H_6–O_2 IT-PCFC at a vertical orientation can deliver enhanced performance when using Pt/BCY15 (thickness = 0.44 mm)/Pt membrane electrode assembly (MEA) and glass sealant (Aremco 617) applied on the anode side. The flow rates of C_2H_6 and O_2 are both kept at $100\,cm^3\,min^{-1}$ during testing. At 650 °C, the maximum power density was enhanced to $116\,mW\,cm^{-2}$ and the corresponding current density was $235\,mA\,cm^{-2}$ in a vertical IT-PCFC (Fig. 4),
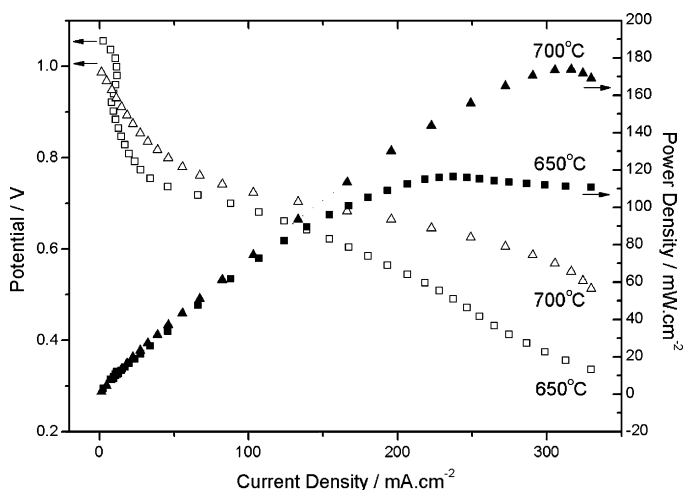

Fig. 4. Current density–voltage (open markers) and current density–power density curves (solid markers) of a C_2H_6–O_2 IT-PCFC with vertical orientation, having BCY15 membrane and Pt paste as both anode and cathode electrodes at 650 °C (squares) and 700 °C (triangles). The flow rates of C_2H_6 and O_2 were both $100\,cm^3\,min^{-1}$.

much higher than that of $21\,mW\,cm^{-2}$ and $58\,mA\,cm^{-2}$ in a horizontal orientation using ceramic sealant [18]. Accordingly, the ethane conversion and ethylene selectivity improved to 30% and 97%, respectively. At 700 °C, the maximum power density and the corresponding current density improved to $174\,mW\,cm^{-2}$ and $320\,mA\,cm^{-2}$, respectively, again much higher than that of $56\,mW\,cm^{-2}$ and $164\,mA\,cm^{-2}$ for the horizontal set-up. Also, both ethane conversion and ethylene selectivity were enhanced to 34% and 96%, respectively. The high ethane conversion and ethylene selectivity showed the advantage of an IT-PCFC reactor for C_2H_6 conversion to C_2H_4, compared with catalytic oxidative dehydrogenation of ethane to ethylene on chromium oxide or nickel oxide based catalysts [23,24].

It is noteworthy that no acetylene was detected in the effluent from the anode chamber. The divergence from 100% selectivity therefore arose from formation of coke and other unidentified by-products. Consequently, we are investigating modifications to the catalyst and its environment with the objectives of reducing coking while avoiding formation of unwanted by-products. In parallel, we are modifying operating parameters to enhance conversion toward commercially viable levels without deleteriously affecting selectivity.

3.5. Enhancement of performance of IT-PCFC

When using the vertical design of the C_2H_6–O_2 IT-PCFC, two of the factors contributing to the improvement of cell performance compared to other tests were (i) excellent sealing performance of glass sealant, and (ii) thinner BCY15 membrane (thickness = 0.44 mm).

We found in preliminary experiments that several ceramic sealants were unsuitable for use with ca. 0.5 mm BCY15 membranes, as they were very prone to cracking, detached from the membranes, or compromised the physical integrity of the membrane surfaces. As discussed in the literature, glass sealant heated to 850 °C can provide an excellent gas-tight seal [15]. We have now shown using SEM micrograph of glass sealant coating formed after heating to 871 °C that a well-bonded contiguous and dense layer is formed without any holes or cracks (Fig. 5A). EDS analysis identified the bar-shaped crystalline phase (point 1 in Fig. 5A) as $CaSiO_3$ (Fig. 5B), and the composition of non-crystalline phase (point 2 in Fig. 5A) was Na_2O–K_2O–CaO–SiO_2 composites (Fig. 5C). The more amorphous phase extended between the crystallites to form a more dense seal. Bansal and Gamble showed that a glass sealant of composition $35BaO$–$15CaO$–$5Al_2O_3$–$10B_2O_3$–$35SiO_2$ (mol%) does not fully crystallize even after long term heat treatment at 750–900 °C [16]. When calcined, the ceramic sealant composed of alumina phosphates was shown by EDS (Fig. 6B) to be a porous assemblage of small particles 2–7 μm (Fig. 6A), which resulted in detrimental effects caused by continuous leakage of small amounts of air into the anode chamber, producing undesirable carbon oxides. Therefore, it is preferable to use calcined glass sealant which forms a dense and gas impermeable coating suitable for fuel chambers of hydrocarbon IT-PCFC. However,
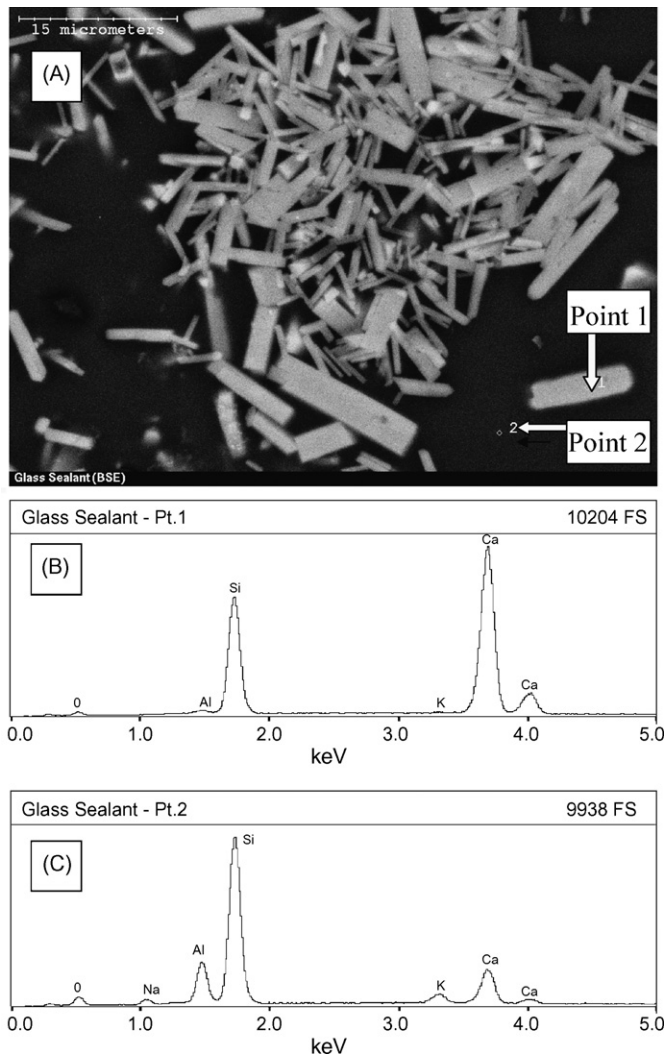
Fig. 5. (A) Scanning electron microscopy (SEM) and (B and C) energy-dispersive X-ray spectroscopy (EDS) analysis of glass sealant (Aremco 617) scratched from the fuel cell set-up after fuel cell tests at high temperature. (B) EDS of point 1 in Fig. 7A. (C) EDS of point 2 in Fig. 7A.

as shown in Section 3.4, the glass sealant cannot be subjected to torsional strain.

EIS of a single SOFC often reveals electrolyte resistance, indicated by the intersection on the real axis, and electrode polarization resistance indicated by the succeeding semi-circle [25]. When using a thin (0.44 mm) BCY15 membrane instead of a 1 mm BCY15 membrane as electrolyte and Pt paste as electrodes at both sides in an IT-PCFC, the electrolyte resistances were reduced to 3.2 and 2.8 Ω cm^2 at 650 and 700 °C (Fig. 7), respectively, thus significantly improving cell performance. The rise in electrode polarization resistance from 2.7 to 4.2 Ω cm^2 tested at 650 °C first and then at 700 °C is caused by coke accumulation over the anode when heating from 650 to 700 °C and during stabilizing at 700 °C, as is well known from hydrocarbon cracking reactions. Therefore it is important to find effective electro-catalysts for dehydrogenation of C_2H_6 without coking in a C_2H_6–O_2 IT-PCFC. It is also important to develop supported thinner film proton-conducting electrolytes to further improve cell performance.
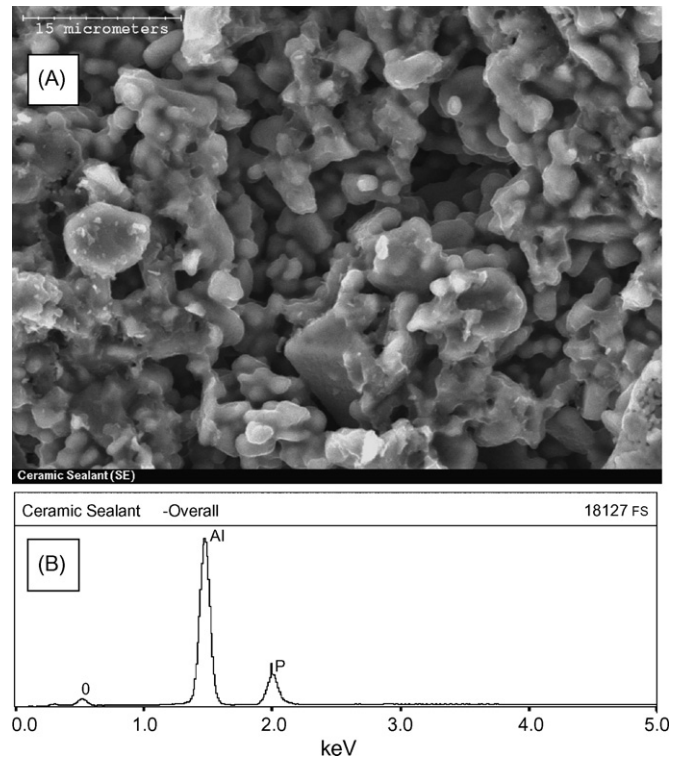
Fig. 6. (A) Scanning electron microscopy (SEM) and (B) overall energy-dispersive X-ray spectroscopy (EDS) analysis of ceramic sealant (Aremco 503) scratched from the fuel cell set-up after high temperature test.
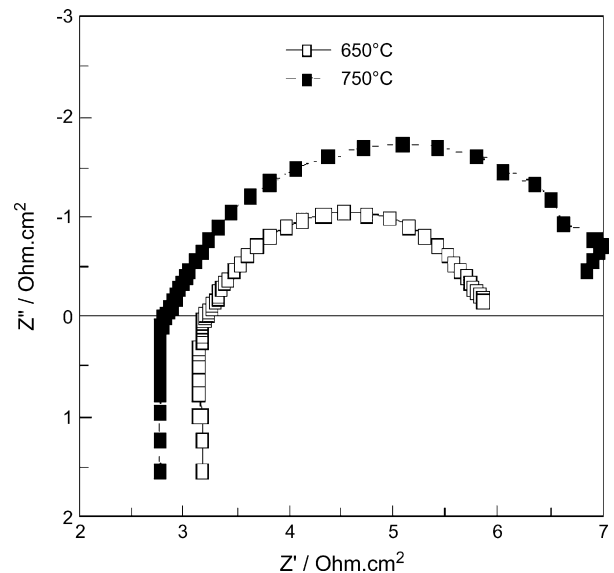

Fig. 7. Electrochemical impedance spectra (EIS) of a C_2H_6–O_2 IT-PCFC having a vertical orientation with BCY15 membrane as electrolyte (thickness = 0.44 mm) and Pt paste as both anode and cathode electrodes at 650 (open squares) and 700 °C (solid squares). The flow rates of C_2H_6 and O_2 were both 100 cm^3 min^{-1}.

4. Conclusions

Proton-conducting perovskite $BaCe_{0.85}Y_{0.15}O_{3-\alpha}$ (BCY15) membranes showed good conductivity of 15 and 20 mS cm^{-1} at 700 and 750 °C, respectively. A vertically oriented C_2H_6–O_2

IT-PCFC with BCY15 as electrolyte and Pt paste as both electrode catalysts, sealed into place using glass sealant, provided high ethane conversion (34%) with very good ethylene selectivity (96%) at 700 °C with ethane and oxygen flow rates both 100 cm^3 min^{-1}. Maximum power density up to 174 mW cm^{-2} and related current densities up to 320 mA cm^{-2} were achieved. A glass sealant provided enhancement sealing of ca. 0.5 mm BCY15 membranes when compared to other ceramic sealants, and so enhanced cell performance, but only when there was no torsional strain.

Acknowledgements

References

[1] T. Norby, Y. Larring, Curr. Opin. Solid State Mater. Sci. 2 (1997) 593.
[2] K.D. Kreuer, Ann. Rev. Mater. Res. 33 (2003) 333.
[3] J. Wang, X. Su, R. Liu, Y. Hu, Y. Xie, F. Yue, Prog. Chem. 16 (2004) 828.
[4] A. Atkinson, S. Barnett, R.J. Gorte, J.T.S. Irvine, A.J. McEvoy, M. Mogensen, S.C. Singhal, J. Vohs, Nat. Mater. 3 (2004) 17.
[5] W.G. Coors, J. Power Sources 118 (2003) 150.
[6] T. Norby, M. WiderØe, R. Glöckner, Y. Larring, Dalton Trans. 19 (2004) 3012.
[7] D. Shima, S.M. Haile, Solid State Ionics 97 (1997) 443.
[8] N. Bonanos, K.S. Knight, B. Ellis, Solid State Ionics 79 (1995) 161.
[9] S. Gopalan, A.V. Virkar, J. Electrochem. Soc. 140 (1993) 1060.
[10] M.J. Scholten, J. Schoonman, J.C. Miltenburg, H.A.J. Oonk, Solid State Ionics 61 (1993) 83.
[11] N. Bonanos, B. Ellis, M.N. Mahmood, Solid State Ionics 44 (1991) 305.
[12] S.V. Bhide, A.V. Virkar, J. Electrochem. Soc. 146 (1999) 4386.
[13] C.D. Savaniu, J. Canales-Vazquez, J.T.S. Irvine, J. Mater. Chem. 15 (2005) 598.
[14] M.J. Pascual, V.V. Kharton, E. Tsipis, A.A. Yaremchenko, C. Lara, A. Durán, J.R. Frade, J. Eur. Ceram. Soc. 26 (2006) 3315.
[15] S.M. Gross, T. Koppitz, J. Remmel, J.B. Bouche, U. Reisgen, Fuel Cells Bull. (2006) 12.
[16] N.P. Bansal, E.A. Gamble, J. Power Sources 147 (2005) 107.
[17] M. Liu, P. He, J.L. Luo, A.R. Sanger, K.T. Chuang, J. Power Sources 94 (2001) 20.
[18] S. Wang, J.L. Luo, A.R. Sanger, K.T. Chuang, J. Phys. Chem. C 111 (2007) 5069.
[19] K.D. Kreuer, Solid State Ionics 97 (1997) 1.
[20] B.C.T. Steele, A. Heinzel, Nature 414 (2001) 345.
[21] U.S. Department of Energy, Fuel Cell Handbook, 6th ed., EG&G Technical Services Inc., 2002, Chapter 7, p. 3.
[22] W. Suksamai, I.S. Metcalfe, Solid State Ionics 178 (2007) 627.
[23] S. Deng, H. Li, Y. Zhang, Chin. J. Catal. 24 (2003) 744.
[24] Y. Wu, T. Chen, X. Cao, W. Weng, J. Zhang, H. Wan, Acta Chim. Sin. 62 (2004) 1678.
[25] Z. Xu, J. Luo, K.T. Chuang, J. Electrochem. Soc. 154 (2007) B523.